Theoretical and experimental investigation of compatible SSB modulation for single channel long-distance optical OFDM transmission

Yuanyuan Zhang[1], Maurice O'Sullivan[2], and Rongqing Hui[1*]

[1]Department of Electrical Engineering and Computer Science, the University of Kansas, Lawrence KS, 66045, USA
[2] *Ciena Inc., Ottawa Carling Campus, 3500 Carling Ave., Nepean, ON, K2H 8E9 Canada*
rhui@ku.edu

Abstract: We present the first experimental demonstration of compatible single-sideband (compatible-SSB) modulated OFDM optical system at 11.1Gb/s data rate for long distance transmission over 675km uncompensated standard single-mode fiber. Compatible-SSB modulation employing a simple dual-drive Mach-Zehnder modulator (MZM) in the transmitter and direct-detection at the receiver provides an OFDM system implementation with reduced complexity. It does not require a guard-band between the carrier and the OFDM sideband and so makes full use of available digital-to-analog converter (DAC) bandwidth. We demonstrate digital pre-compensation applied in the transmitter to correct MZM nonlinear transfer function and to improve the system transmission performance. We show that optimum modulation index value decreases with increasing transmission distance. We have also investigated the impact of self-phase modulation (SPM) on the system performance, and show that a compatible-SSB modulated system is less vulnerable to SPM in comparison to the conventional offset-SSB modulation at the same data rate.

©2010 Optical Society of America

OCIS codes: (060.0060) Fiber optics and optical communications; (250.0250) Optoelectronics.

References and links

1. R. Hui, B. Zhu, R. Huang, C. Allen, K. Demarest, and D. Richards, "Sub-carrier multiplexing for high-speed optical transmission," J. Lightwave Technol. **20**(3), 417–427 (2002).
2. R. Hui, "Multi-tributary OFDM optical transmitter using carrier-suppressed optical single-sideband modulation" Proceedings of Optical Fiber Communication Conference; OFC'2003, paper MF74, Atlanta, GA, March 2003.
3. N. E. Jolley, H. Kee, R. Rickard, J. Tang, and K. Cordina, "Generation and propagation of a 1550nm 10Gb/s optical orthogonal frequency division multiplexed signal over 1000m of multimode fibre using a directly modulated DFB," Proceedings of Optical Fiber Communication Conference, OFC'2005, Paper OFP3.
4. A. J. Lowery, and J. Armstrong, "Orthogonal-frequency-division multiplexing for dispersion compensation of long-haul optical systems," Opt. Express **14**(6), 2079–2084 (2006).
5. W. Shieh, and C. Athaudage, "Coherent optical orthogonal frequency division multiplexing," Electron. Lett. **42**(10), 587–589 (2006).
6. I. B. Djordjevic, and B. Vasic, "Orthogonal frequency division multiplexing for high-speed optical transmission," Opt. Express **14**(9), 3767–3775 (2006).
7. P. J. Winzer, and R.-J. Essiambre, "Advanced Modulation Formats for High-Capacity Optical Transport Networks," J. Lightwave Technol. **24**(12), 4711–4728 (2006).
8. M. Schuster, S. Randel, C. A. Bunge, S. C. J. Lee, F. Breyer, B. Spinnler, and K. Petermann, "Spectrally efficient compatible single-sideband modulation for OFDM transmission with direct detection," IEEE Photon. Technol. Lett. **20**(9), 670–672 (2008).
9. W.-R. Peng, X. Wu, K.-M. Feng, V. R. Arbab, B. Shamee, J.-Y. Yang, L. C. Christen, A. E. Willner, and S. Chi, "Spectrally efficient direct-detected OFDM transmission employing an iterative estimation and cancellation technique," Opt. Express **17**(11), 9099–9111 (2009).
10. B. J. C. Schmidt, A. J. Lowery, and L. B. Du, "Low Sample Rate Transmitter for Direct-Detection Optical OFDM" Proceedings of Optical Fiber Communication Conference, OFC 2009, San Diego, CA, paper OWM4.
11. Z. Xu, M. O'Sullivan, and R. Hui, "OFDM system implementation using compatible SSB modulation with a dual-electrode MZM," Opt. Lett. **35**(8), 1221–1223 (2010).

12. J. McNicol, M. O'Sullivan, K. Roberts, A. Comeau, D. McGhan, and L. Strawczynski, "Electrical Domain Compensation of Optical Dispersion," Proceedings of Optical Fiber Communication Conference, OFC'2005, Anaheim, CA, paper OThJ3.
13. K. Roberts, C. Li, L. Strawczynski, M. O'Sullivan, and I. Hardcastle, "Electronic pre-compensation of optical nonlinearity," IEEE Photon. Technol. Lett. **18**(2), 403–405 (2006).
14. R. Hui, and M. O'Sullivan, "*Fiber Optic Measurement Techniques*," Academic Press, 2009.
15. Y. Benlachtar, G. Gavioli, V. Mikhailov, and R. I. Killey, "Experimental investigation of SPM in long-haul direct-detection OFDM systems," Opt. Express **16**(20), 15477–15482 (2008).

1. Introduction

Multi-carrier modulation has demonstrated potential for use in long-distance optical fiber transmission. A high data rate digital signal can be partitioned into multiple subcarriers where the data rate on each subcarrier can be sufficiently low as to significantly improve tolerance to transmission degradations such as chromatic dispersion and polarization mode dispersion [1,2]. The rapid recent progress in development of high-speed digital electronic circuits including (analog-to-digital converter) ADC and (digital-to-analog converter) DAC, has made possible orthogonal frequency-division multiplexing (OFDM) in high-speed optical systems, in which multiple subcarriers are created in digital domain and guard bands between adjacent subcarrier channels are no longer required [3–6]. In addition to the increase of optical bandwidth efficiency, digital signal processing (DSP) techniques can be applied to reduce inter-symbol interference through equalization before and/or after transmission. OFDM is a well-studied digital modulation method which supports advanced electrical and optical modulation formats and relies on DSP [7] to achieve higher spectral efficiency and better system performance for high-speed optical transmission. OFDM optical systems with both coherent-detection and direct-detection have been demonstrated with single sideband (SSB) optical spectrum to reduce the impact of fiber chromatic dispersion [3–6]. While coherent OFDM systems provide better spectral selectivity and receiver sensitivity, direct detection systems are simpler without a local optical oscillator and its associated stabilization and phase/polarization diversity apparatus.

In an OFDM system with direct detection, signal subcarriers in the optical domain are down-converted into RF domain by mixing with the optical carrier at the photodiode. At the same time, subcarrier channels within the same OFDM band also mix with each other to generate crosstalk. To avoid this signal-signal beat interference (SSBI), a guard-band between the optical carrier and the OFDM subcarriers (with the same bandwidth as the OFDM signal) is usually reserved [4]. This design is commonly referred to as offset–SSB modulation. It not only reduces the bandwidth efficiency, but also wastes approximately 50% of the DAC and ADC capabilities in the transmitter and the receiver. These deficiencies are addressed by encoding the information into the exponential envelope of the optical signal [8], which eliminated the nonlinear mixing among OFDM channels on photo-detection, and any need for a guard-band to separate the optical carrier from OFDM subcarriers. This compatible-SSB modulation has the least complexity in comparison with other techniques which remove the guard-band [9, 10]. A straightforward implementation of an optical SSB OFDM transmitter can be a simple intensity modulator and a narrowband optical filter to select one from the two redundant optical sidebands. Other implementations use a Hilbert transform in both the RF and the optical domains to suppress the unwanted optical sideband. Although, an optical in-phase/quadrature-phase (I/Q) modulator can directly translate complex RF signals into the optical domain [8], a more traditional dual-drive Mach-Zehnder modulator (MZM) can also be used with appropriate digital signal processing to obtain real-valued electrical signals to drive the two modulator arms [11].

This paper presents a systemic theoretical and experimental investigation of compatible-SSB modulation in long-distance optical OFDM transmission. The system uses a traditional dual-drive MZM transmitter and a direct-detection receiver. A commercial optical transmitter originally designed for 10 Gb/s binary optical transmission with electrical-domain pre-compensation (eDCO) [12, 13] is used, which is equipped with two 22.2Gs/s DACs and a dual-drive MZM. Although an I/Q modulator has been previously suggested for a compatible-

SSB system [8], we show that a simple dual-drive MZM provides comparable performance for this particular modulation format. We demonstrate that system transmission performance can be improved by appropriate digital pre-compensation in the transmitter to correct the nonlinear transfer characteristics of the MZM. We have performed detailed analysis on the impact of the MZM bias variation and the optical modulation index. The results indicate that high modulation index is preferred for noise limited systems, whereas a lower modulation index is required for uncompensated long-distance systems possessing large chromatic dispersion. The impact of nonlinear SPM has also been investigated in this system. Because compatible-SSB modulation eliminates the requirement of the guard-band between the carrier and the OFDM signal sideband, the overall optical bandwidth is 50% narrower than the offset-SSB modulated OFDM system of the same data-rate, and as a consequence, the tolerance to nonlinear SPM is also improved.

2. Principle of operation

In general, an OFDM optical field can be expressed by a summation of a central optical carrier and multiple signal subcarriers,

$$\tilde{x}(t) = A_0 \left[1 + \sum_{k=0}^{N-1} \tilde{X}_k \exp\left(j2\pi k \Delta f t \right) \right] \cdot e^{j\omega_0 t} \tag{1}$$

Where, ω_0 is the optical carrier frequency, A_0 is the optical carrier amplitude, N is the total number of subcarrier channels and Δf is the frequency spacing between adjacent channels. $\tilde{X}_k = A_k e^{j\theta_k}$ is the normalized complex QPSK/QAM data symbol on the k-th carrier with A_k and θ_k representing the magnitude and the phase, respectively. Therefore, the bandwidth of the OFDM spectrum is $N \cdot \Delta f$.

At the optical receiver, the photo-detector performs square-law detection, and the photocurrent is proportional to the received optical power:

$$\tilde{i}(t) = \eta \left| A_0 \right|^2 \left| 1 + \sum_{k=0}^{N-1} \tilde{X}_k \exp\left(j2\pi k \Delta f t \right) \right|^2 \tag{2}$$

Where, η is the photo-detector responsivity. While the useful RF spectrum comes from the mixing between the optical carrier and the OFDM subcarriers whose amplitude is proportional to $\tilde{X}_k$, mixing also happens among subcarrier channels producing crosstalk with the amplitude proportional to $\tilde{X}_i \tilde{X}_j$ ($i, j = 1, 2 \ldots N$). The frequency of this inter-mixing crosstalk spreads over the RF bandwidth between DC and $N \cdot \Delta f$. To avoid contamination of the OFDM signal by this signal-signal beat interference, the OFDM signal subcarriers are offset to higher frequencies to introduce a guard-band between the optical carrier and the signal sideband. Figure 1 illustrates the optical and electrical spectra of the offset-SSB modulation for an OFDM system in which the 6GHz guard-band is equal to the OFDM signal sideband. It can be seen that, after direct detection, the guard-band in the electrical domain is filled with signal-signal beat interference noise. The need for a guard-band reduces the spectral efficiency by a factor of 2. Also, the DAC in the transmitter has to have twice the bandwidth of the OFDM signal, which imposes an upper limit on the overall data rate the transmitter can support.

Compatible-SSB modulation encodes the OFDM data onto the exponential envelope of the optical field, which can be expressed as,

$$\tilde{x}(t) = A_0 \exp\left[\sum_{k=0}^{N-1} \tilde{X}_k \exp\left(j2\pi k \Delta f t \right) \right] \cdot e^{j\omega_0 t} \tag{3}$$

After the square-law detection in an optical receiver, the photocurrent is,

$$\tilde{i}(t) = \eta |A_0|^2 \exp\left\{ 2 \sum_{k=0}^{N-1} \tilde{X}_k \exp\left(j2\pi k \Delta ft \right) \right\} \qquad (4)$$
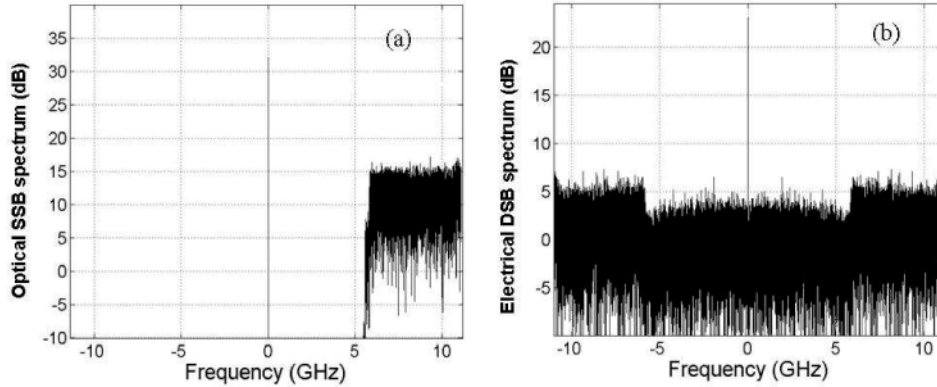

Fig. 1. Spectra of offset-SSB modulation (a) optical single-sideband spectrum, and (b) electrical double-sideband spectrum after square law detection

This avoids the nonlinear mixing among the OFDM subcarriers in the detection process as illustrated by Fig. 2. Theoretically, the original OFDM signal can be recovered by simply applying a nature log operation, while in practice, small-signal linearization can be used to simplify the recovery process. Therefore, with compatible-SSB modulation and direct detection, a guard-band is not needed, and the OFDM signal can occupy the entire DAC bandwidth starting from almost DC.
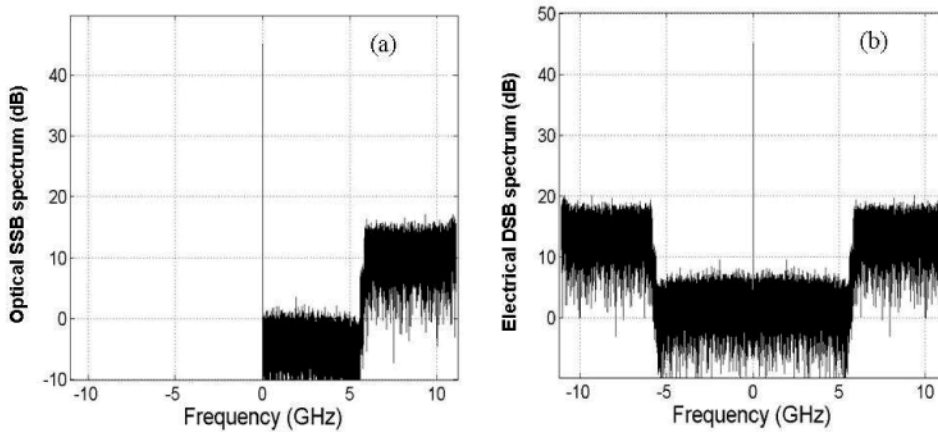

Fig. 2. Spectra of compatible-SSB modulation (a) optical single-sideband spectrum, and (b) electrical double-sideband spectrum after square law detection.

The optical signal of compatible-SSB modulation can be generated through an ideal I/Q modulator, which directly translates the complex electrical waveform into optical domain [8]. However, since the OFDM signal is encoded as an exponential term as indicated in Eq. (3), the negative part of the optical field envelope cannot be explored. Given this, one can use a simple dual-drive MZM without loss of functionality and at some reduction of cost and complexity.

In order to derive the voltage drive waveforms for the dual-electrode MZM, we assume that the OFDM signal in the electrical domain is $\sigma(t) = \sum_{k=0}^{N-1} \tilde{X}_k \exp\left(j2\pi k \Delta ft \right)$. To convert $\sigma(t)$

into single sideband, we create another waveform $m(t) = \sigma(t) + jH[\sigma(t)]$, where $H[\ ]$ denotes Hilbert transform. For compatible-SSB optical modulation, this single-sideband electrical signal is carried as an exponential term in the optical signal, which is,

$$n(t) = \exp[m(t)] = A(t)e^{j\Phi(t)} \tag{5}$$

The amplitude and phase of this optical signal is related to the original OFDM signal by [8],

$$A(t) = \exp[\sigma(t)] \tag{6}$$

and

$$\Phi(t) = H[\sigma(t)] = H\{\ln[A(t)]\} \tag{7}$$

For an ideally linearized modulator with two balanced electrodes, the intensity modulation is proportional to the differential phase between the two arms, while the phase modulation is proportional to the common-mode phase of the two arms. Therefore, the optical signal required for compatible-SSB transmitter can be obtained through,

$$\frac{\phi_1(t) - \phi_2(t)}{2} \cdot \exp\left[j\frac{\phi_1(t) + \phi_2(t)}{2} \right] = A(t)e^{j\Phi(t)} \tag{8}$$

The optical phases φ_1 and φ_2 of the two modulator arms should be [9],

$$\phi_1(t) = \Phi(t) + A(t) \tag{9a}$$

$$\phi_2(t) = \Phi(t) - A(t) \tag{9b}$$

For practical dual-drive MZM biased at the quardrature point, the transfer function between the CW input optical field E_i and output optical field $E_0(t)$ is not perfectly linear,

$$E_0(t) = 2E_i \sin\left[\Delta\phi(t) + \frac{\pi}{4} \right] \exp j\left[\phi_0(t) - \frac{\pi}{4} \right] \tag{10}$$

Where, $\phi_0(t) = \pi[v_1(t) + v_2(t)]/2V_\pi$, $\Delta\phi(t) = \pi[v_1(t) - v_2(t)]/2V_\pi$ are the common-mode and differential phase delay of the two MZM arms, respectively. $v_1(t)$ and $v_2(t)$ are electrical signal voltage applied on the two electrodes, and V_π is the voltage for a π phase shift in the MZM power transfer function.

To take this nonlinear intensity transfer characteristic into account, the required electrical signals on the two MZM electrodes should be,

$$v_1(t) = \frac{V_\pi}{\pi}\left\{ \Phi(t) + \sin^{-1}(A(t)) \right\} \tag{11a}$$

$$v_2(t) = \frac{V_\pi}{\pi}\left\{ \Phi(t) - \sin^{-1}(A(t)) + \pi/2 \right\} \tag{11b}$$

Unlike using an ideal I/Q modulator where the complex RF spectrum is linearly translated into the optical domain [8], in a practical system using a dual-drive MZM, both modulation index and the accuracy of bias setting are important parameters affecting system transmission performance. A small modulation index can ensure the linear operation and avoid the clipping from the MZM. But if the modulation index is too small the signal sideband will have much lower power than that of the carrier, and therefore the system will be vulnerable to optical noise. On the other hand, a high modulation index will explore the nonlinear transfer function of the MZM, and clipping will happen at the peak intensity of the OFDM signal. The interaction between these nonlinear modulation effects and the chromatic dispersion in the

transmission fiber will further distort the waveform and introduce transmission performance degradation. Therefore, the optimal MZM modulation index usually depends on the fiber characteristics and the transmission distance of the system.
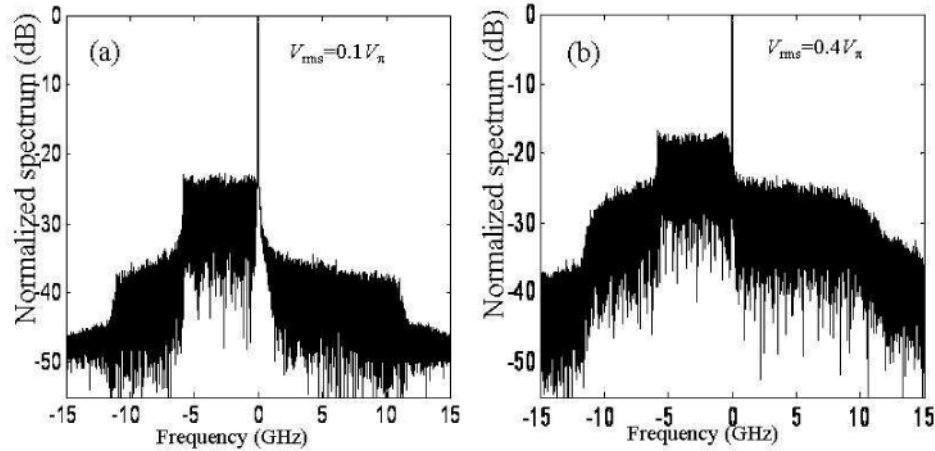

Fig. 3. Optical spectra of compatible-SSB OFDM signal with small modulation index (a) and large modulation index (b).

For a noise-limited system, higher modulation index can help to reduce the carrier-to-signal power ratio and thus improve the system performance. Whereas if the system is limited by the chromatic dispersion, the modulation index cannot be too high, otherwise the sideband suppression ratio of the signal will deteriorate and high-order harmonics will increase in the spectrum. Figure 3 shows two examples of optical spectra with low and high optical modulation indices. Obviously, increasing the modulation index from 10% to 40%, the power in the OFDM sideband increases by 6dB, but at the same time, frequency components at high-order harmonics, as well as in the image sideband, are increased dramatically due to the nonlinear transfer function and clipping of the MZM, and therefore the system will become vulnerable to chromatic dispersion in the system. Throughout this paper, the modulation index is defined as the RMS voltage of the OFDM signal divided by the V_π of the modulator.

3. Experimental setup

In order to experimentally investigate the compatible-SSB modulated OFDM system for long-distance fiber-optic transmission, we assembled a transmission test-bed using an optical re-circulating loop. Figure 4 shows the block diagram of the experimental setup. The OFDM signal is generated by an offline program in MATLAB. An 11.1 Gb/s serial data is mapped onto QAM-4 format, and loaded onto 64 subcarriers by serial-to-parallel conversion. We have used $N = 256$ block in the IFFT operation, in which the OFDM subcarriers occupy inputs 1 – 64 while the complex conjugate of the OFDM subcarriers are loaded into inputs 193 – 256 in a reverse sequence. This data mapping insures that the time-domain signal has real values after the IFFT operation. Inputs 65 – 192 are padded with zeros to fill up the entire 256 IFFT block. This provides 2 times oversampling, which takes 4 samples per OFDM period using the 22.2 GS/s DAC. Two training symbols are inserted at the beginning of the OFDM symbol for timing synchronization and digital equalization.

A commercial optical transmitter provided by CIENA Inc is used, which was initially designed for 10 Gb/s binary optical transmission with electrical-domain pre-compensation (eDCO) [12,13]. This eDCO card is equipped with two DACs with 22.2Gs/s sampling speed at 6-bits resolution and a 2^{15}-long memory, so that it functions as a 22.2 Gs/s dual-channel arbitrary waveform generator (AWG). The card is also imbedded with a tunable laser and a balanced duel-drive MZM. By loading the digitally-created OFDM data into the eDCO memory, the compatible-SSB optical signal can be obtained.
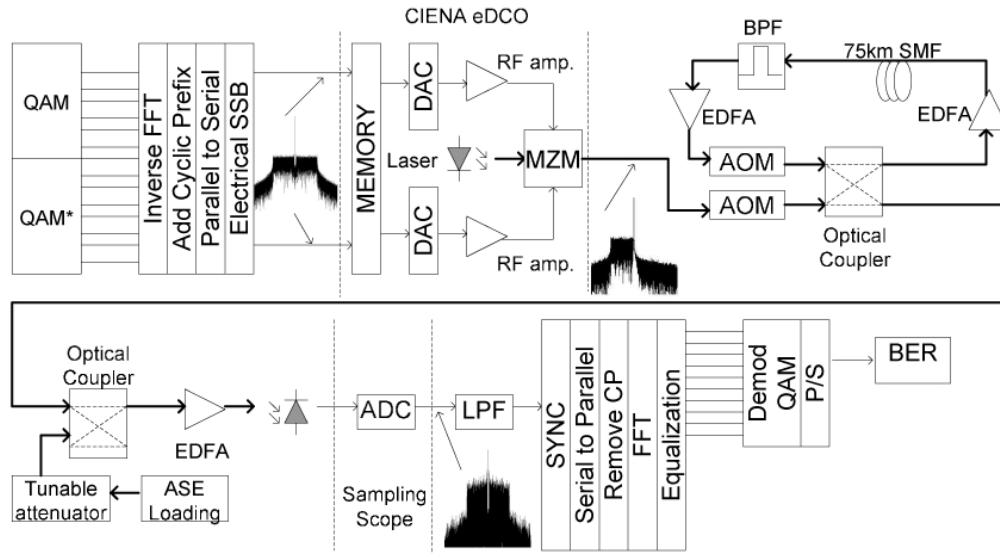
Fig. 4. Experimental setup

To test the long-distance transmission performance, a fiber-optic re-circulating loop is used in the system. Each span of the loop consists of 75km uncompensated standard single-mode fiber (SMF), two in-line EDFAs, and a 1-nm bandwidth tunable optical filter to prevent saturation of the in-line EDFAs by the accumulated ASE noise. At the output of the re-circulating loop, another EDFA is used as a pre-amplifier to boost the signal optical power before it reaches the photodiode. The electrical signal output from the photodiode is sampled and recorded by a real-time oscilloscope (LeCroy 8600A) which has 20 Gs/s sampling rate and 6 GHz analog bandwidth. Receiver signal-processing functions, including synchronization, cyclic prefix removal, FFT, and equalization are performed offline in a MATLAB program. In order to evaluate the required optical signal to noise ratio (R-OSNR) for different system configurations and settings, noise loading is used in the experiment, in which a controllable amount of ASE noise generated by an EDFA without input is added to the optical signal at the receiver by an optical coupler.

It is worthwhile to note that with QAM-4 data format using compatible-SSB modulation, the 11.1 Gb/s data signal only occupies approximately 5.5GHz electrical bandwidth, which determines the required analog bandwidth of the DAC. The spectrum of the recovered RF signal at the receiver is illustrated in Fig. 4, which has 5.5GHz bandwidth on each side of the DC. While this eDCO transmitter card with 22.2GS/s DAC speed is capable of delivering 22.2 Gb/s data rate, our system capacity is primarily limited by the real-time oscilloscope at the receiver which only has 6GHz analog bandwidth. As a comparison, if an IQ modulator was used in the system, the required DAC bandwidth may be halved by shifting the center of the electrical SSB signal to zero frequency [8]. However, for compatible-SSB optical modulation, since the optical field has to be positive (as exponential envelop), the use of an IQ modulator would not help to reduce the required DC component to improve the carrier-to-signal power ratio (CSPR).

4. Results and discussion

Based on the operation principle described in section 2 and the system configuration discussed in section 3, we have also compiled a numerical simulation tool to investigate the properties of optical OFDM systems using compatible-SSB modulation. The transmitter model uses the same parameters as those in the experiment, with 6-bits DAC at the sampling rate of 22.2Gs/s. The fiber transmission model uses a split-step Fourier analysis which includes chromatic dispersion and Kerr effect nonlinearity in the fiber. The comparison

between measured results and those from numerical simulations provides help to better understand mechanisms of various system degradation effects, as well as ways to optimize the system.

4.1 MZM bias and nonlinear equalization

As discussed in the previous section, a practical MZM has nonlinear transfer characteristics. Driving waveforms given by Eq. (9) derived from the linear approximation of the MZM transfer function [9] may introduce waveform distortions. Thanks to the digital implementation of the transmitter, this nonlinear transfer function can be pre-compensated by using the driving waveforms defined by Eq. (11). Figure 5 shows the measured BER versus OSNR characteristics for a back-to-back OFDM system. In the experiment, digital signal was pre-clipped such that the peak amplitude of the OFDM waveform is 4.62 time its root-mean-square (*rms*) value. This value was chosen based on the analysis provided in [8]. Less clipping would result in high DC level in the signal and thus high CSPR, whereas stronger clipping would cause intolerable signal bit errors even before transmission. Without nonlinear pre-compensation, the MZM operates in linear regime only when the modulation index is small enough. Nonlinear pre-compensation relaxes this restriction to some extent and allows the use of higher modulation indices. Without applying the nonlinear pre-compensation, the required OSNR to achieve a BER of 10^{-3} is approximately 22dB and optimum modulation index is $0.2V_\pi$. With nonlinear pre-compensation, a higher modulation index of $0.3V_\pi$ can be used for the optimum system performance, and the required OSNR to achieve a BER of 10^{-3} is improved by 4dB to approximately 18dB. The two constellation diagrams in Fig. 5 were examples measured at 20dB OSNR level, with and without the nonlinear pre-equalization.
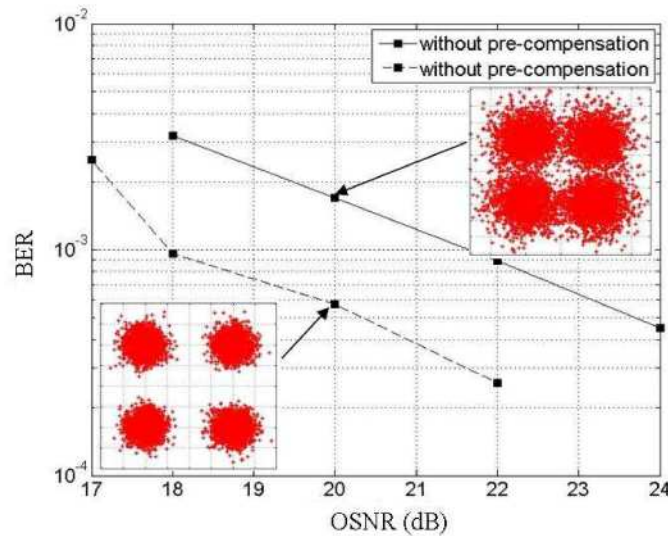

Fig. 5. BER versus signal OSNR in a back-to-back system with and without nonlinear pre-compensation of MZM transfer function.

For a practical electro-optic modulator based on a dual-drive Mach-Zehnder interferometer, besides the correction of nonlinear transfer function, proper DC bias is another important issue to optimize the system performance.

In a dual-drive MZM, the generation of optical single-sideband modulation requires the bias level to be at the quadrature point [1,14]. The system performance sensitivity to the level of MZM biasing is an important parameter in practical system implementation, which determines whether a precise feedback control is required. Figure 6 (a) shows the measured BER versus the normalized MZM bias voltage variation for back-to-back (stars) and over 3 fiber spans (open circles) OFDM systems. In the diagram, zero normalized bias voltage

means the modulator is biased at the quadrature point. MZM nonlinearity pre-compensation was added in the transmitter. For the back-to-back measurement the modulation index on the MZM was about $0.3V_\pi$ and the signal OSNR was 20dB, while in the measurement of the 3-span system, the modulation index was $0.2V_\pi$, and the OSNR was about 24dB. Figure 6 (b) shows the results of numerical simulation for the same systems, but the OSNR had to be 14dB for the back-to-back system and 20dB for the 3-span system to obtain the comparable BER levels with the experiments. Nevertheless, both the measured and the simulated BER curves indicate that the optimum bias level of the MZM changes for approximately 10% between the back-to-back system and the system with 3 spans of standard SMF. The reason can be explained as follows: For back-to-back experiment, chromatic dispersion is negligible, and the deterioration of sideband suppression ratio caused by moving the bias away from the quadrature point does not significantly degrade transmission performance. This allows the bias to be set at a lower transmission point so that the power in the carrier can be reduced, and thus the reduction of carrier-to-signal ratio. On the other hand, for a long-distance transmission over fiber with significant chromatic dispersion, optical sideband suppression ratio has to be high enough to avoid the crosstalk between the two sidebands at the receiver. In this case, the bias has to be set sufficiently close to the quadrature point. In both cases, the normalized bias voltage variation has to be kept within $< \pm 5\%$ for negligible BER degradation.
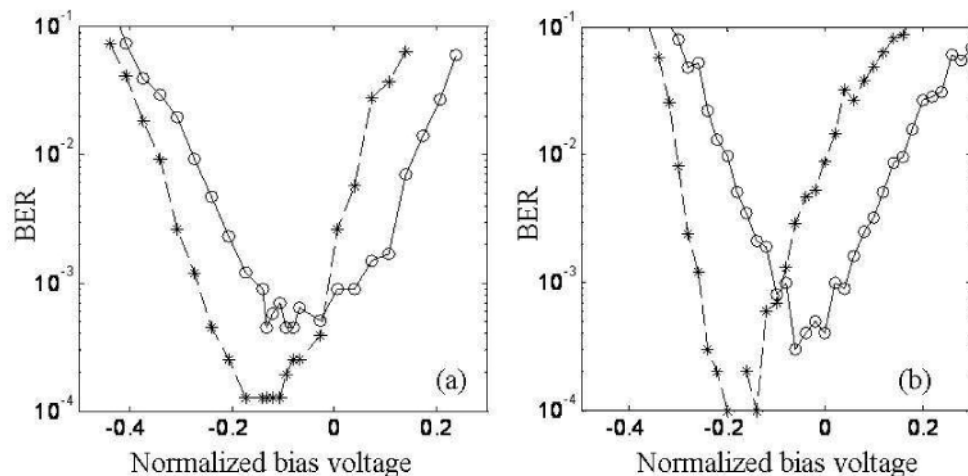

Fig. 6. BER versus normalized bias voltage variation from the quadrature point for back-to-back (stars) and over three fiber spans (open circles). (a) measured and (b) numerical simulation

4.2 Impact of MZM modulation index

In addition to the bias level and the pre-equalization of MZM nonlinear transfer function, modulation index is another important parameter critical to the system transmission performance. Figure 7 (a) shows the measured BER as the function of the MZM modulation index in a re-circulating loop experiment. It is worth noting that for back-to-back system without optical fiber involved, the optimum modulation index is around 30%. When transmission fiber is introduced with significant chromatic dispersion, the optimum modulation index becomes much smaller at about 10%, and in this case the CSPR of the optical signal is approximately 7dB. This reduced optimum modulation index in long distance system is primarily due to the requirement of high sideband suppression ratio of SSB modulation. At high modulation index, although the carrier-to-signal ratio can be improved to some extent, the rise of the unwanted optical sideband as illustrated in Fig. 3 reduces the system tolerance to chromatic dispersion. The result of numerical simulation shown in Fig. 7 (b) qualitatively agrees with the measurements, except in Fig. 7(a) the optimum modulation

index is slightly smaller in the system with 15 spans in comparison to the case of 9 spans, which might be due to experimental uncertainties and the selection of sampling points in the experiment.
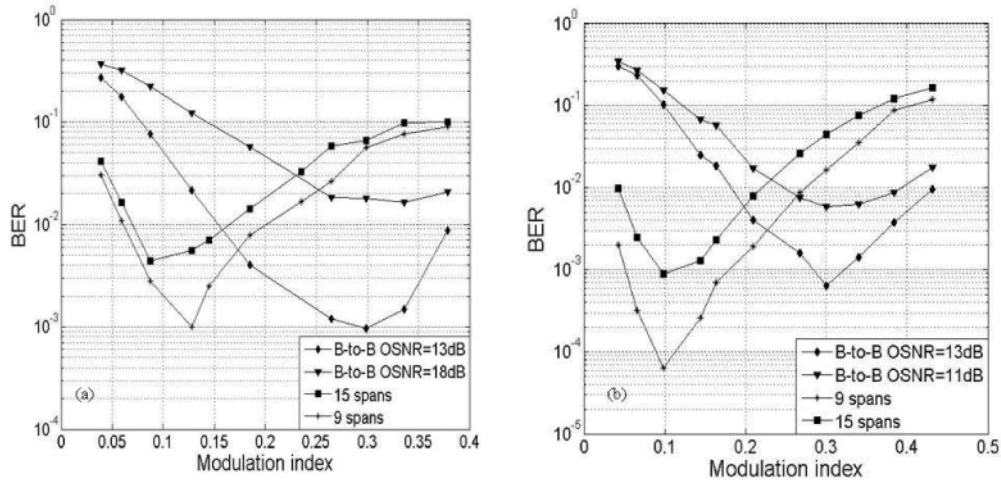

Fig. 7. BER versus MZM modulation index. (a) experiment, and (b) simulation. Modulation index is defined as the *rms* driving signal voltage divided by V_π.

Figure 8 shows the optimum modulation index as the function of the number of uncompensated fiber spans (75km standard SMF per span) obtained by more systematic numerical simulations. The OSNR level at the receiver was kept at 17dB in the simulation. The optimal modulation index reduces significantly over the first five spans, which is roughly equivalent to the dispersion length of the signal with 5GHz bandwidth over standard SMF. Further decrease the modulation index will not bring additional improvement on the sideband suppression ratio in the SSB modulation while only deteriorates (increase) the carrier-to-noise ratio. A tradeoff has to be made between minimizing the dispersion-induced crosstalk and maximizing the power in the OFDM sideband.
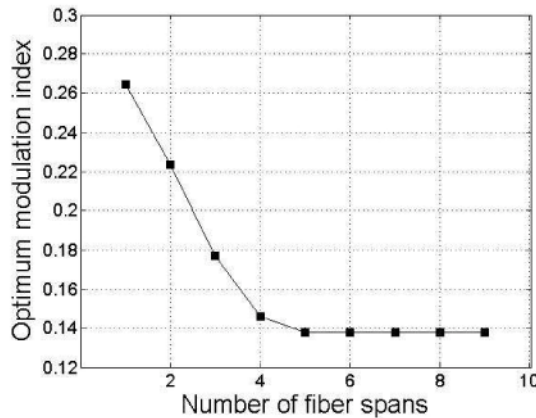

Fig. 8. Simulated optimum modulation index as the function of fiber length. Modulation index is defined as the *rms* driving signal voltage divided by V_π.

4.3, Required OSNR

For long-distance optical transmission over amplified fiber spans, one of the most important parameters is the required OSNR to achieve the pre-FEC BER of 10^{-3}. Figure 9 shows measured and simulated BER versus OSNR characteristics of the 11.1 Gb/s compatible-SSB

system for back-to-back and over different numbers of uncompensated fiber spans. The measurement was performed using an optical re-circulating loop setup as described in section 3. The roundtrip optical loss in each loop is approximately 28dB, which includes 16dB loss for 75km standard SMF, and losses from optical coupler (3dB), band-pass optical filter (2dB) and an acousto-optic switch (7dB). Optical noise loading was used before the receiver to measure the BER as the function of signal OSNR.
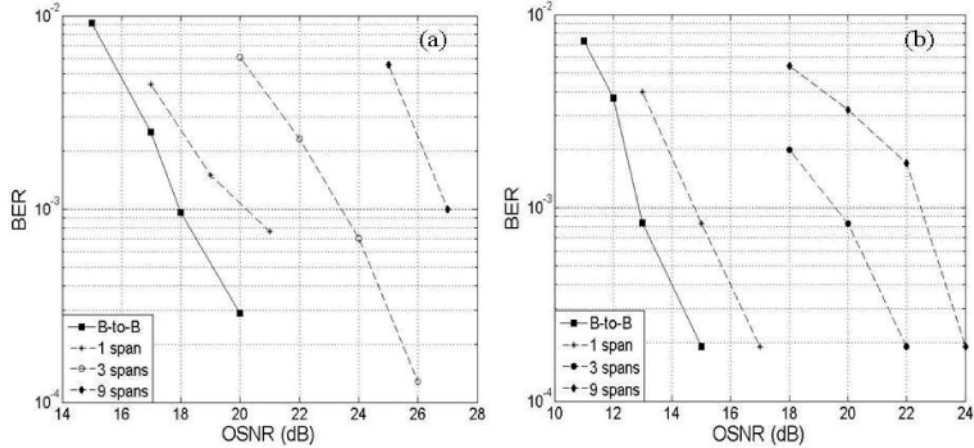

Fig. 9. BER versus OSNR for different transmission distances. (a) measured and (b) numerical simulation

Figure 10 summarizes the required OSNR (R-OSNR) for BER = 10^{-3} as a function of the system fiber length. There is an approximately 5 dB difference between the measured R-OSNR and the results of numerical simulation using the same parameters. This discrepancy can be attributed to imperfections in the experimental systems, such as multipath optical and RF interferences along the system which create ripples in the transfer functions. In fact, a computer simulation indicated that approximately 1-dB ripple in the overall system transfer function may introduce 1-dB OSNR penalty in the system performance. There is an approximately 9dB OSNR penalty after 675km transmission over the fiber compared to back-to-back. Part of the reason is due to the high modulation index used for short distance transmission which has to be reduced for long distances. The maximum transmission distance here is primarily limited by the achievable OSNR of 27dB after 9 fiber spans in the re-circulating loop. A longer transmission distance may be possible in a real multi-span optical system in which there is no extra insertion loss in each span as in the re-circulating loop system and thus the OSNR level will be higher.
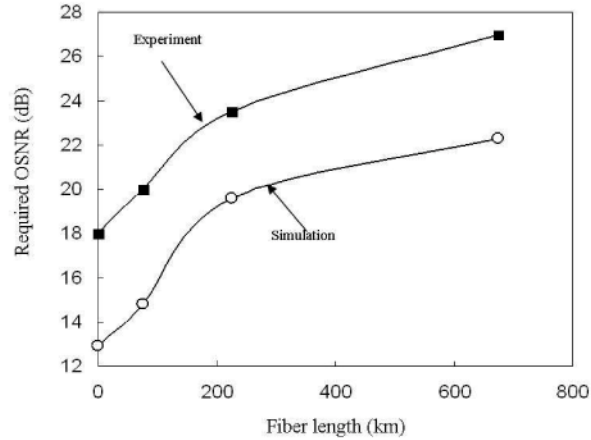
Fig. 10. Required OSNR versus fiber length.

5. Impact of self-phase modulation

A general concern in OFDM modulation format is its high peak-to-average ratio for the signal, and therefore transmission systems using OFDM might be vulnerable to fiber nonlinear effects such as self-phase modulation (SPM) [15]. Although it is an important parameter, the sensitivity to SPM has not been investigated so far for the OFDM system based on compatible-SSB modulation.

Our SPM measurement was performed in the same re-circulating loop setup discussed in section 3. The launched optical power into the transmission fiber was varied by changing the saturation level of the in-line EDFA in the loop through the pump power adjustment. Because in the re-circulating loop, the optical loss is fully compensated by the EDFA gain, the launched power into transmission fiber is expected to be the same for every span. Figure 11 shows the BER measured after 9 spans of fiber transmission as the function of the launched optical power, and throughout the measurement, the receiver OSNR was kept at about 27dB. The results shown in Fig. 11 indicate that, except for a small fluctuation, BER is generally not sensitive to the launched optical power when its level is lower than 4.5dBm. Rapid BER degradation is observed when the power level is beyond 5dBm. A numerical simulation was also performed based on the experimental system configuration and uses a split-step Fourier method. The parameters used in the simulation are: fiber length of each span $L = 75$ km, fiber attenuation parameter $\alpha = 0.21$ dB/km, nonlinear refractive index $n_2 = 2.35$ m^2/W, fiber core effective area $A_{eff} = 80\mu$m^2, and fiber dispersion coefficient $D = 16$ ps/nm·km at the signal wavelength of $\lambda = 1547$nm. In order for the BER to be comparable to the experiment, the OSNR at the receiver was kept at 23dB in the simulation. The result from numerical simulation, also shown in Fig. 11 as open circles, agrees reasonably well with the experiment.
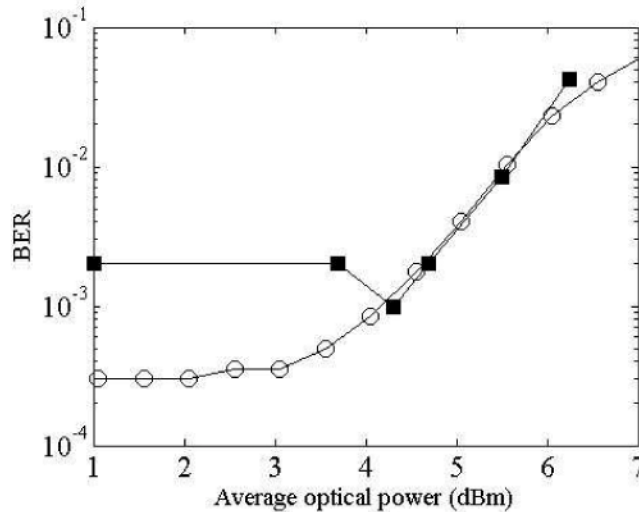
Fig. 11. Measured (solid squares) and simulated (open circles) BER versus launch power for compatible-SSB OFDM system after 675km fiber transmission

SPM performance in OFDM system with direct detection has been previously measured using standard offset-SSB modulation at the data rate of 11.1 Gb/s [15]. The system performance was found to degrade by SPM significantly when the launched optical power approaches 0dBm. Figure 11 indicates that for the same data rate, an OFDM using compatible-SSB modulation is much less sensitive to the impact of SPM. There are two major reasons for this reduced SPM sensitivity. The first reason is the reduced optical spectral bandwidth of compatible-SSB modulation. For 11.1 Gb/s data rate, standard offset-SSB modulation requires the modulation bandwidth of approximately 11.5 GHz because of the required guard-band between the carrier and the OFDM sideband. Since this guard band is not necessary in compatible-SSB format, its optical bandwidth is only half in comparison to the offset-SSB modulation. It is well known that SPM-induced optical frequency chirp is proportional to the time derivative of the signal power [14]. This nonlinear frequency chirp is converted into an intensity crosstalk through chromatic dispersion in the transmission fiber. The impact of this extra intensity crosstalk in the system performance is proportional to the optical bandwidth of the signal. Therefore, part of the SPM tolerance improvement should be attributed to the signal bandwidth change from 11.5GHz (for offset-SSB modulation) to 5.75GHz (for compatible-SSB modulation). The second reason for the decreased SPM sensitivity of compatible-SSB modulated system is the relatively small modulation index and thus the high carrier-to-signal ratio. Because the OFDM signal is encoded in the exponential envelope of the optical carrier, the average power represented by the carrier component is generally high in comparison to offset-SSB modulation.

It is also worth noting that although the system using compatible-SSB modulation is less sensitive to the effect of SPM, other nonlinear effects, such as cross-phase modulation and four-wave mixing, may set the upper power limit in WDM optical systems using this modulation format due to inter-channel crosstalk. This is beyond the scope of this investigation.

6. Conclusion

We have performed a systemic investigation of compatible-SSB modulated OFDM system for single channel long-distance optical transmission. The simple system configuration using direct-detection, and the elimination of the guard-band requirement makes this modulation format attractive for low-cost implementation. We have experimentally demonstrated a compatible-SSB modulated OFDM system with 11.1 Gb/s data rate based on a standard dual-

drive MZM in the transmitter, and an optical transmission over 675km uncompensated standard SMF in an optical re-circulating loop. We have investigated various issues in system performance optimization, which include digital pre-compensation of the MZM nonlinearity transfer function, optimum bias level and modulation index and their dependence on system transmission distance. We have also measured the impact of nonlinear SPM in the transmission performance, and demonstrated the improved SPM tolerance of compatible-SSB modulated OFDM system compared to its offset-SSB counterpart at the same data rate. The results of our numerical simulation based on split-step Fourier method agree reasonably well with the experiments, which helped to understand the physical mechanisms behind the measured results.

By modulating the signal in the exponential envelop of the optical carrier, Compatible-SSB modulation has the advantage of improved spectral efficiency in comparison to the offset-SSB modulation. However, as a drawback, the relatively high DC component in the Compatible-SSB signal increases the CSPR which increases the required OSNR in the receiver.

Acknowledgements